Available online at www.sciencedirect.com
SCIENCE DIRECT®
Polymer 44 (2003) 6617–6625
polymer
www.elsevier.com/locate/polymer

Crystallization behavior and morphology of poly(ethylene 2,6-naphthalate)

Wan Duk Lee[a], Eui Sang Yoo[b], Seung Soon Im[a,*]

[a]*Department of Fiber and Polymer Engineering, College of Engineering, Hanyang University, 17 Haengdang-dong, Seongdong-gu, Seoul 133-791, South Korea*
[b]*Polymer Science and Engineering, University of Massachusetts Amherst, Amherst, MA 01003, USA*

Received 10 June 2003; received in revised form 7 August 2003; accepted 8 August 2003

Abstract

The crystallization behavior and morphology of poly(ethylene 2,6-naphthalte) (PEN) were investigated by means of differential scanning calorimetry (DSC), polarized optical microscopy (POM) and transmission electron microscopy (TEM). POM results revealed that PEN crystallized at 240 °C shows the coexistence of α and β-form spherulite morphology with different growth rates. In particular, when PEN crystallized at 250 °C, the morphology of spherulites showed a squeezed peanut shape. The Avrami exponents decreased from 3 to 2.8 above the crystallization temperature of 220 °C, indicating a decrease in growth dimension. Analysis from the secondary nucleation theory suggests that PEN crystallized at 240 °C has crystals with both regime I and regime II. In TEM observation, the ultra-thin PEN film crystallized at 200 °C showed the spherulitic texture with characteristic diffractions of α-form, while PEN crystallized at 240 °C generated an axialite structure with only β-form diffraction patterns. In addition, despite a long crystallization time of 24 h, amorphous regions were also observed in the same specimen. It was inferred that the initiation of PEN at 240 °C generates only β-form crystals from axialite structures.

Keywords: Poly(ethylene 2,6-naphthalate); Crystal polymorphism; Crystallization kinetics

1. Introduction

Resulting from increased chain stiffness, poly(ethylene 2,6-naphthalate) (PEN) is used as a high-performance polymer that has superior strength, heat stability, and barrier properties [1,2]. Thus, PEN has found for a variety of applications, such as tire cords of automobiles [3] and base films of videotapes [4], etc.

It has been reported that PEN has two polymorphs, α and β-form, depending on the crystallization conditions such as crystallization temperature and pre-melting temperature [5–7]. The unit cell of the α-form was determined by Mencik [5] as triclinic ($a = 0.651$ nm, $b = 0.575$ nm, $c = 1.32$ nm, $\alpha = 81.33°$, $\beta = 144°$, $\gamma = 100°$). The other crystal modification, β-form, is determined by Zachmann et al. [6]. It is also triclinic with the following unit cell parameters: $a = 0.926$ nm, $b = 1.559$ nm, $c = 1.273$ nm, $\alpha = 121.6°$, $\beta = 95.57°$, $\gamma = 122.52°$. Recently, some researchers reported another crystal form (γ-form), a four chain monoclinic unit cell [16,17].

Fairly many studies on the crystallization of PEN have been reported to date, including crystalline structure [5–7], crystallization kinetics [7], liquid-induced crystallization [8], structural change/formation during uniaxial [9–12] or biaxial drawing [9], and crystal morphology [13–16]. However the origin of the two basic crystal forms has not been reported clearly, although Buchner et al. [7] analyzed the formation of the α and β-forms by considering fluctuation of the crystal embryos in the melting state.

In the present study, the crystallization behavior and morphology of PEN during isothermal crystallization were investigated by means of differential scanning calorimetry (DSC), polarized optical microscopy (POM) and transmission electron microscopy (TEM). In particular, this study focused on the growth of both crystal forms at a relatively high temperature of 240 °C by analyzing crystallization kinetics and morphology results.

* Corresponding author. Tel.: +82-2-2290-0495; fax: +82-2-2297-5859.
E-mail address: kaitei@dreamwiz.com (W.D. Lee), imss007@hanyang.ac.kr (S.S. Im).

0032-3861/$ - see front matter © 2003 Elsevier Ltd. All rights reserved.
doi:10.1016/j.polymer.2003.08.002

2. Experimental

2.1. Material

PEN chips were kindly supplied by Kolon Co. Ltd. The intrinsic viscosity (IV) of PEN chips measured in a 60/40 (wt%) mixture of phenol and tetrachloroethane was 0.44 dl g^{-1}. This value of IV was relatively low because the PEN chips used in the present study were raw products before solid-state polymerization. The chips were dried in a vacuum oven at 120 °C for 24 h prior to use.

2.2. Measurements

The thermal characteristics of PEN, including crystallization exotherms, were measured using a Perkin–Elmer DSC 7 instrument, previously calibrated with indium and zinc. The polymer sample was heated to 300 °C, kept for 5 min to eliminate thermal history, and then cooled rapidly to the desired crystallization temperature within the range of 200–250 °C. During isothermal crystallization, exothermic heat flow was recorded as a function of time. The fully crystallized sample was quenched to 50 °C, and a second run was carried out.

Morphological observations of PEN spherulites were conducted with a polarized optical microscope (Nikon HFX-11A). A small amount of the sample, sandwiched between slide glass and cover glass, was first melted on a hot plate at 300 °C for 5 min and then rapidly transferred to the hot stage (Mettler Toledo FP82HT) that was equilibrated at the desired isothermal crystallization temperature. With annealing for the required crystallization time, the radial growth rate of spherulites was measured.

To check the crystal form of the PEN, wide-angle X-ray diffraction (WAXD) measurements were carried out on a Rigaku Denki X-ray generator (Rigaku model D/MAX-2500) using Cu Kα radiation operated by 40 kV and 100 mA. The scan angle covered $10° < 2\theta < 35°$ (2θ is scattering angle, θ is Bragg angle) at a speed of 5°/min.

For detailed morphological observations and electron diffraction experiments, a transmission electron microscope (JEOL 2000FX, operated at 200 kV) was carried out. Ultra-thin PEN films were prepared by solution casting. A 0.1 wt% PEN solution in 1,1,1,3,3,3-hexafluoro-2-propanol was prepared at room temperature. A carbon-coated mica sheet was dipped into the solution of 30 °C, and dried at room temperature. It was then transferred to the hot stage (Mettler Toledo FP82HT), and crystallized at the same thermal conditions, mentioned above, for 24 h. Thereafter, the ultra-thin PEN film and carbon bilayer were detached from the mica sheet onto a water surface, and picked up on a copper grid. The specimen on the grid was shadowed with platinum (Pt) to increase the contrast of the image and calibrate electron diffraction patterns. The shadowing angle was $\tan^{-1}(1/3)$.

3. Results and discussion

3.1. POM observation

Fig. 1 shows polarized optical micrographs of PEN, which were melted at 300 °C and crystallized at (a) 200, (b) 210, (c) 220, (d) 230, (e) 240, and (f) 250 °C. Previous studies reported that the α-form is produced at about 200 °C, while β-form crystallizes at higher crystallization temperatures [7]. Fig. 1(a) shows a well-defined spherulitic texture with a clean Maltese cross. With increasing crystallization temperature, however, the Maltese cross became dimmer and finally disappeared. A banded ring structure then developed, which transformed to a fibril structure at higher crystallization temperatures. In addition, Fig. 1(f) exhibits a squeezed peanut type morphology that is observed only in the β-form crystal. This morphological change coincides with the results of Lee [15] and Liu et al. [16]. They reported that the α-form crystal was accompanied by spherulitic growth at lower temperatures. At higher temperature, the spherulites of PEN became the form of a squeezed peanut shape or amoeba-type structure. This amoeba-type morphology is consistent with the results of the TEM study, which will be discussed later.

In particular, we observed some interesting results on the crystallization, which has two different crystal growth rates. Fig. 1(e) shows two different spherulite forms; one is fibril structure and the other is banded ring structure. Therefore, we carefully observed the real-time growth of the spherulites at the crystallization temperature of 240 °C, from the start of the nucleation process, as shown in Fig. 2. Fig. 2(a) shows the beginning of spherulitic growth for the PEN crystals at 240 °C. After 10 min, PEN crystals grow to two different types of spherulite with different growth rates, as shown in Fig. 2(b)–(d). The spherulites of banded ring structure grew about twice faster than those of fibril structure. In addition, the banded ring spherulites were similar to those grown at 230 °C. Fig. 3 shows WAXD profiles of the PEN crystallized at 200 and 240 °C. The spherulites crystallized at 200 °C show the crystalline reflections of the (010), (100), and ($\bar{1}$10) planes (2θ is 15.64, 23.30, and 26.98°, respectively), which are major reflections of the α-form crystal. However, the specimen crystallized at 240 °C has both β-form crystals, with crystalline reflections of ($\bar{1}\bar{1}$1), (020), ($\bar{2}$02), and ($2\bar{4}2$) planes (2θ is 16.44, 18.54, 23.34, and 25.52°, respectively), and a small quantity of α-form (010) reflections ($2\theta =$ 15.64°). Considering these WAXD results and POM observations, it is supposed that PEN crystallized at 240 °C has both α and β-crystal forms. These results will be discussed further using kinetic theories.

3.2. Avrami theory analysis

Fig. 4(a) shows the isothermal crystallization exotherms of PEN at various crystallization temperatures. The relative

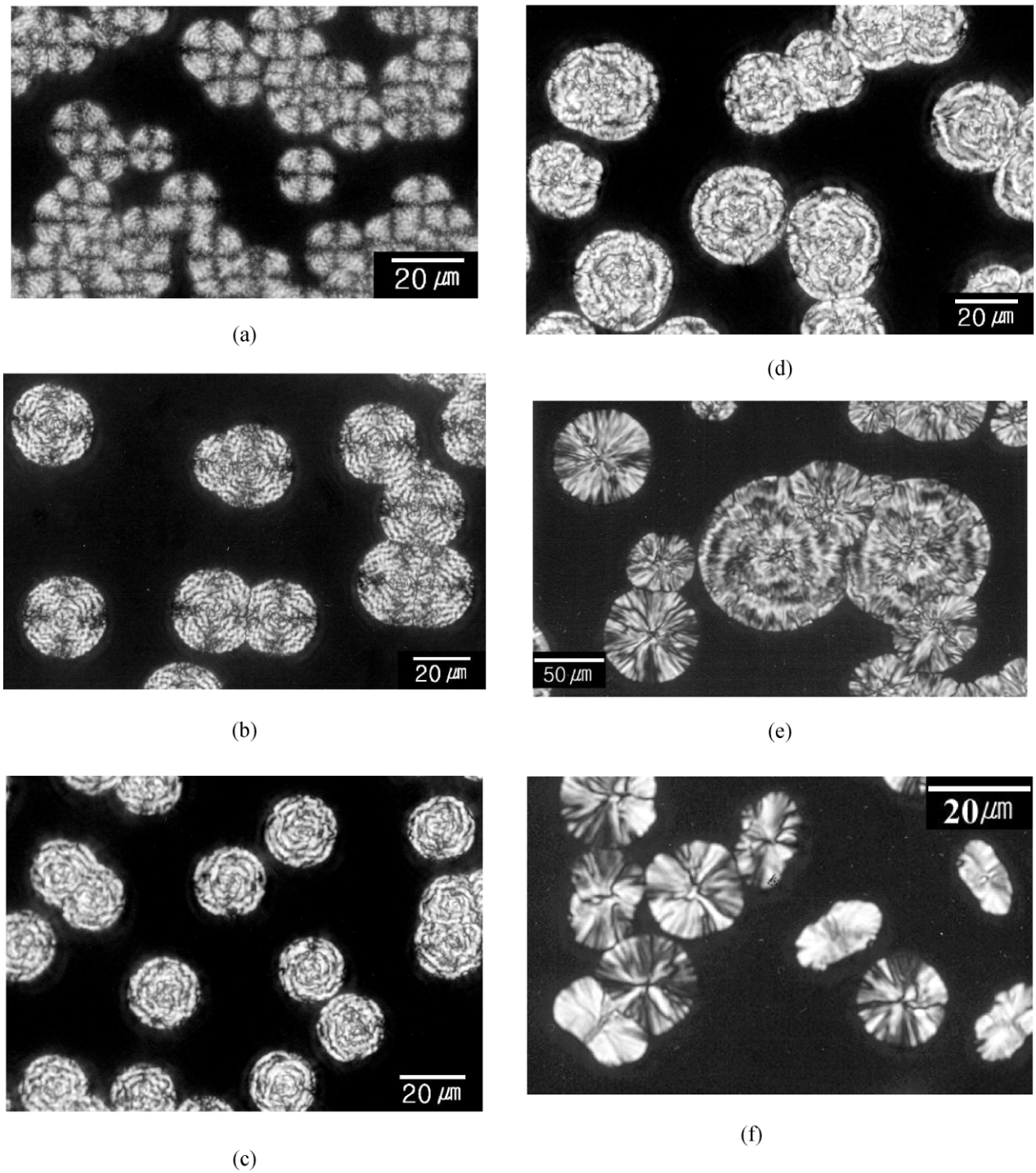

Fig. 1. Polarized optical micrographs of PEN crystallized at (a) 200, (b) 210, (c) 220, (d) 230, (e) 240, and (f) 250 °C.

crystallinity, X_t, was obtained from the ratio of the area of the exotherm up to time t divided by the total exotherm. Fig. 4(b) shows the development of the relative crystallinity with time for PEN. All isotherms exhibited a sigmoidal dependence on time. Above 220 °C, the rate of crystallization conspicuously decreased with increasing crystallization temperature.

The kinetics of crystallization of PEN were analyzed by means of the Avrami equation [19]. The Avrami exponent, n, and rate constant, k, are obtained from the slopes and intercept of the linear plot of $\log(-\ln(1 - X_t))$ against $\ln(t)$ in the primary crystallization portion, respectively. A typical example of Avrami plots for the crystallization behavior of PEN is shown in Fig. 5. With increasing crystallization temperature, the plots shift toward longer times. This reveals that the crystallization rate decreases

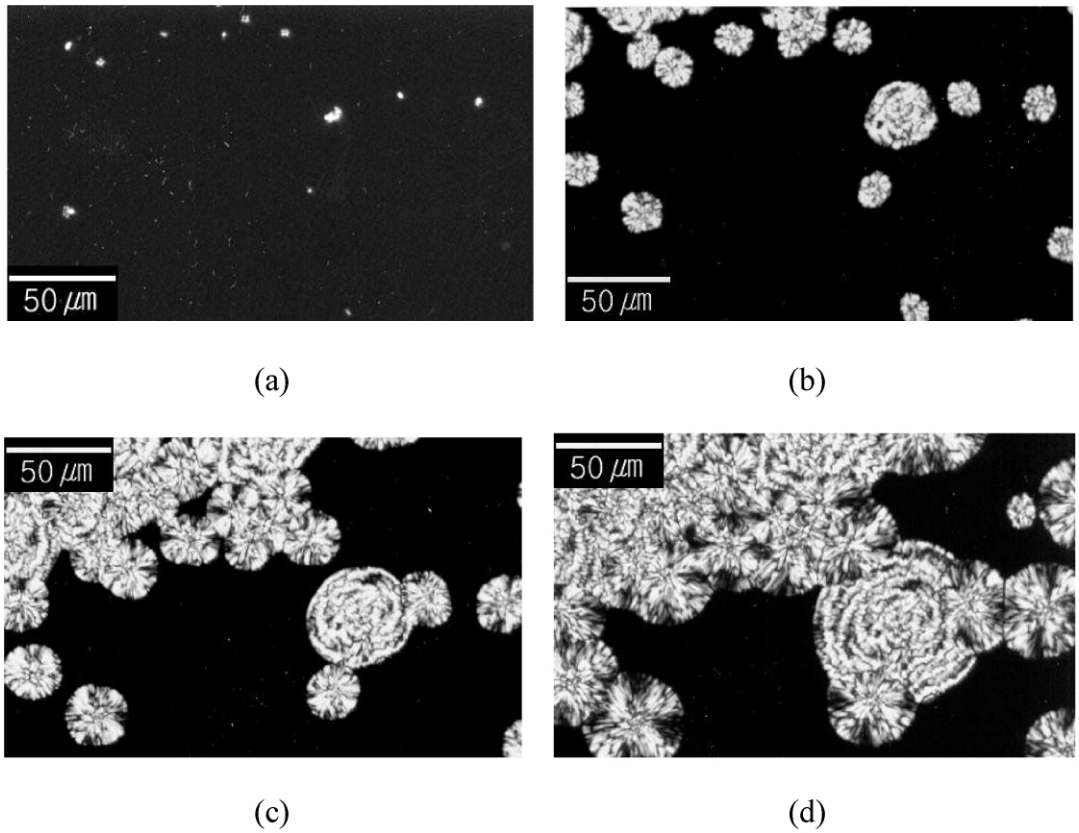

Fig. 2. Polarized optical micrographs of PEN crystallized at 240 °C for (a) 4, (b) 18, (c) 26, and (d) 40 min.

with increasing crystallization temperature. It is clearly observed that the slope of the plots tends to become smaller at high X_t, indicating that secondary crystallization processes take place.

The Avrami kinetic parameters and the half-time of crystallization are listed in Table 1. The half-time of crystallization, $t_{0.5}$, indicating the time for 50% of crystallization was derived from Fig. 4(b). The Avrami exponent n lies in the range of 2.8–3.4. Different n values indicate different nucleation and crystalline growth processes. It is supposed that n values indicate spherical growth with instantaneous nucleation for pure PEN. In addition, the Avrami exponent becomes smaller than 3 above 220 °C. It is supposed that the growth form of PEN crystal deviates from an ideal spherical growth pattern and shows an oval form at a higher crystallization temperature. The data of $t_{0.5}$ and k indicate that the crystallization temperature of 210 °C shows the fastest crystallization rate in the whole crystallization temperature range. Over the 210 °C, $t_{0.5}$ and k show very sensitive decrease of crystallization rate. However, when PEN crystallized at 230 °C, the increment of the half-time of crystallization, equivalent to the decreasing overall crystallization rate, is much more bigger than rate constant decrement. At the same time, the Avrami exponent is abnormally decreased to 3. It is anticipated that the overall crystallization rate is decreased because the crystal growth

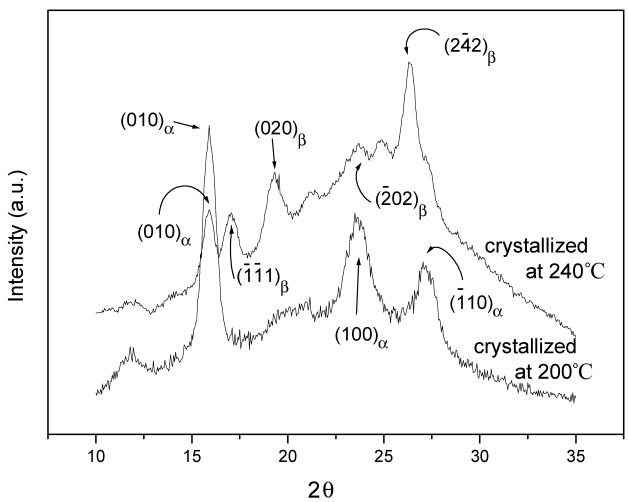

Fig. 3. WAXD curves of PEN crystallized at 190 and 240 °C for about 30 min.

Table 1
Avrami kinetic parameters for the crystallization of PEN

Sample	Crystallization temperature (°C)	$t_{0.5}$ (s)	n	k (s^{-n})
PEN	200	114	3	1.4×10^{-7}
	210	111	3.3	2.1×10^{-7}
	220	117.6	3.4	1.2×10^{-7}
	230	180	3	9.8×10^{-8}
	240	324	2.8	4.1×10^{-8}
	250	960	2.8	8.4×10^{-9}

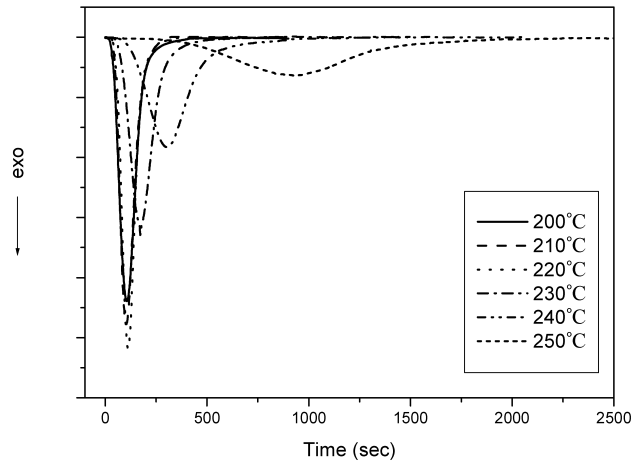

(a)

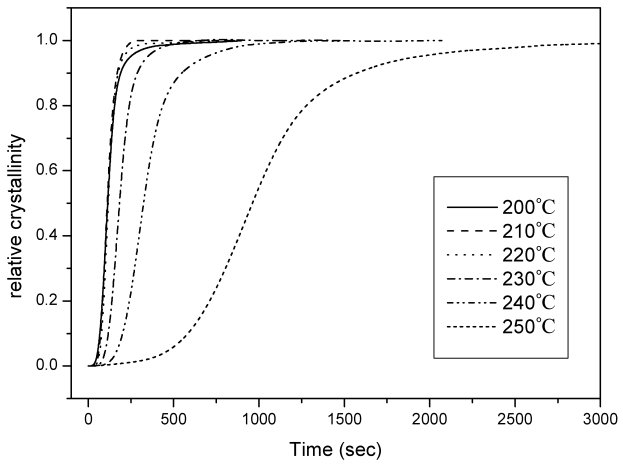

(b)

Fig. 4. (a) DSC isothermogram and (b) relative crystallinity vs. time at various crystallization temperatures for PEN.

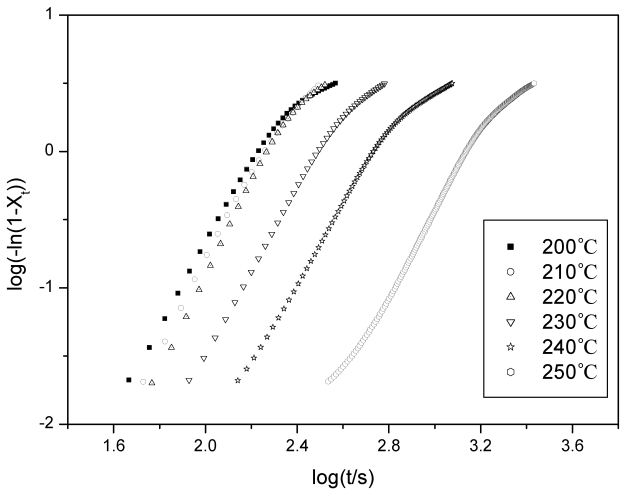

Fig. 5. Avrami plot for PEN.

mechanism might be changed while the nucleation density decreased continuously.

Fig. 6 presents the second-run thermogram for the fully crystallized PEN. For crystallization temperatures up to 230 °C, three melting peaks can be observed. As the crystallization temperature increases above 230 °C, the low and middle melting peaks shift to higher temperatures. In particular, the height of the middle melting peak increases with the crystallization temperature. In contrast, the highest melting peak, which always appears at the same temperature, reduces in height. Above 240 °C, all melting peaks merge to a single peak and shifts to higher temperature. This result is similar to those reported by Cheng and Wunderlich [18]. The small and low endotherm corresponded to the melting of small crystallites formed between main lamellar populations, and the high endotherm corresponded to the melting of crystallites produced by melt-recrystallization. The middle endotherm was attributed to the melting of original crystal lamellae grown during isothermal crystallization. In this work, the equilibrium melting temperature was obtained by application of a Hoffman–Weeks plot to these middle endotherms (Fig. 7). Extrapolation of the middle melting peak with respect to crystallization temperature intersects with the line of $T_m = T_c$ at about 296 °C.

3.3. Secondary nucleation theory

The rates of crystal growth were derived from the slopes of the lines obtained by plotting the spherulite radius against time. For amoeba-type crystals, the distance from the crystal center to the oval having short curvature was measured with time. The growth rate results are shown in Fig. 8. The growth rate decreased with increasing crystallization temperature. In addition, there are two growth rates when PEN crystallized at 240 °C. By adopting nucleation theory [20], the crystal growth rate, G, at crystallization

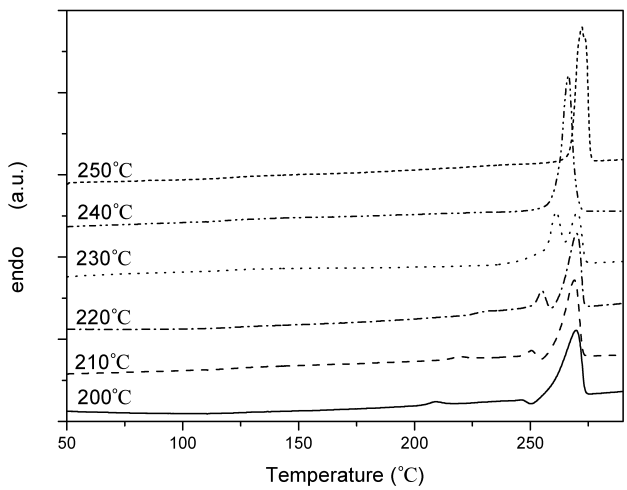

Fig. 6. DSC second run for the fully crystallized PEN at various temperatures.

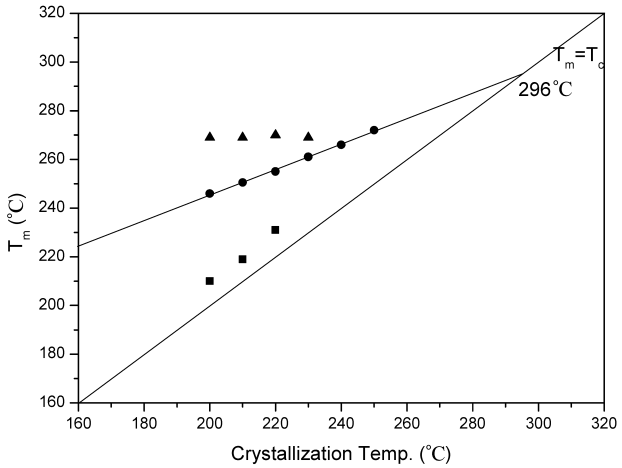

Fig. 7. Hoffman–Weeks plot for PEN.

temperature can be expressed by following equation:

$$G = G_0 \exp\left(-\frac{U^*}{R(T_c - T_\infty)}\right)\exp\left(-\frac{K_g}{T_c(\Delta T)f}\right) \quad (1)$$

where G_0 is the front factor, U^* is the activation energy for the segment diffusion to the site of crystallization, R is the gas constant, T_∞ is the hypothetical temperature below which all viscous flow ceases, K_g is the nucleation parameter, ΔT is the degree of supercooling defined as $T_m^0 - T_c$ and f is a correction factor given as $2T_c/(T_m^0 + T_c)$. Generally, it is convenient to rewrite Eq. (1) in a logarithmic form as follows:

$$\ln G + \left(\frac{U^*}{R(T_c - T_\infty)}\right) = \ln G_0 - \frac{K_g}{T_c(\Delta T)f} \quad (2)$$

Then we plotted $\ln G + U^*/R(T_c - T_\infty)$ against $1/T_c(\Delta T)f$ as shown in Fig. 9. In this work, we used the 'universal' values of $U^* = 6300\ \mathrm{J\ mol^{-1}}$ and $T_\infty = T_g - 30\ \mathrm{K}$ in all calculations [20]. With this assumption, the values of K_g were obtained from the slope of linear fits to the data. As shown in Fig. 9, it clearly exhibits classical regime I → II

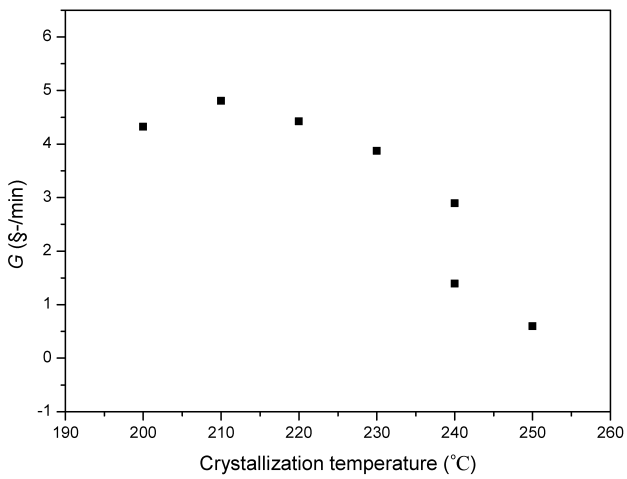

Fig. 8. Plot of crystal growth rate of PEN as a function of crystallization temperature.

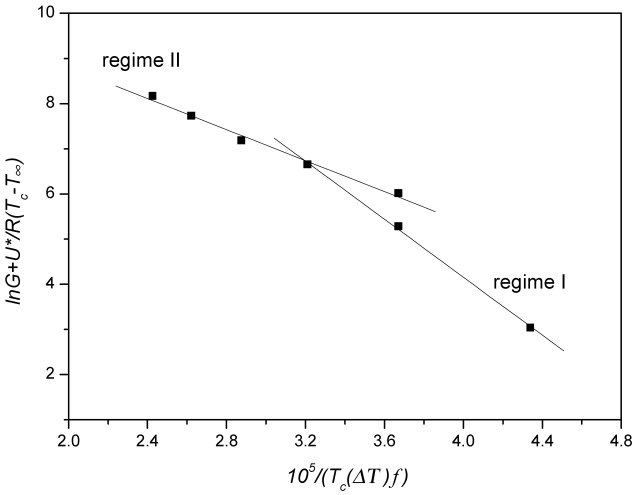

Fig. 9. Plots of $\ln G + U^*/R(T_c - T_\infty)$ against $1/T_c\Delta Tf$ for PEN.

transitions at around 230 °C. The K_{gI}/K_{gII} value in PEN was ca. 1.87, which is close to the theoretical predicted value of 2. In particular, two calculated values obtained from both growth rates at 240 °C were linearly well fitted in the region of two regimes. These results indicate that PEN crystallized at 240 °C has both crystals grown with regime I and regime II. In addition, it is well known that regime I type crystallization exhibits axialitic crystal structure, while regime II type crystallization shows spherulitic morphology. Therefore, combining our POM observations and these kinetic results, it is anticipated that when PEN crystallized at 240 °C spherulites with banded structure are the α-form crystal and those of fibril structure are the β-form crystal.

The nucleation parameter K_g is given by:

$$K_g = \frac{nb_0\sigma\sigma_e T_m^0}{\Delta h_f k_B} \quad (3)$$

where n is a constant equals to 4 for regime I and III and 2 for regime II, b_0 is the molecular layer thickness, σ is the lateral surface energy, σ_e is the fold surface free energy, Δh_f is the heat of fusion per unit volume and k_B is the Boltzmann constant. Here, it should be mentioned that we assumed β-form crystals grow at the regime I region and regime II region allow to grow α-form crystals, discussed above. Therefore, we used different input parameters for the calculation of the surface free energy $\sigma\sigma_e$. The monomolecular layer thickness, b_0 value, of the α-form was taken as the d-spacing of the (010) plane, because Tsuji et al. [14] suggested that the crystallites (α-form) in the two-dimensional spherulite are oriented with their (010) planes being parallel in the radial direction of the spherulite. We also assumed that the β-from crystal is oriented in a similar manner as the α-form. In addition, it was reported that the β-form crystal structure has four chains per unit cell, while the α-form has one chain. Therefore, the monomolecular layer thickness, b_0, of the β-form was taken as the d-spacing of the (020) plane.

On the other hand, the lateral surface free energy, σ was commonly estimated as [20,21]:

$$\sigma = \alpha(\Delta h_f)(a_0 b_0)^{0.5} \quad (4)$$

where, α was derived empirically to be 0.11 by analogy with the well-known behavior of hydrocarbons [22]. a_0 and b_0 factors are the monomolecular width and layer thickness, respectively. In the same manner as discussed above, the a_0 value of the β-form was estimated to the half value of a unit cell dimension and that of α-form was directly used the a parameter of unit cell. The input data and the results obtained from the secondary nucleation analysis are listed in Table 2. It has been known that the greater the fold surface free energy is relative to lateral surface free energy, the more fibrous will be the shape of the nucleus [23]. As seen in Table 2, the value of σ_e respect to the σ value in regime I is greater than that in regime II, indicating that the nucleus shape of the β-form in regime I is more fibrous than that of the α-form in regime II.

3.4. TEM observation

The structural appearance of spherulites observed by POM should be assumed to appear in ultra-thin PEN films crystallized under the same thermal conditions. Fig. 10(a) shows TEM images of the ultra-thin PEN film, melted at 300 °C and crystallized isothermally at 200 °C for 24 h. Fine curved fibrillar entities radiate from the assuming center of spherulite. Fig. 10(b) presents a typical electron diffraction pattern taken from a few spherulites in the same specimen. The outer ring in the pattern comes from the (111) plane of Pt, which was used as a reference to calibrate the distance between camera and specimen. All specimens crystallized 200 °C revealed the same patterns as shown in Fig. 10(b). All of the reflections are major diffractions of the α-form crystals. The crystalline reflection of the (010) plane is clearly observed, and those of the (100) and ($\bar{1}$10) planes are observed indistinctly.

Table 2
Kinetic data for crystallized PEN calculated from secondary nucleation theory

	Regime I	Regime II
$K_g \times 10^5$ (K^2)	3.21	1.72
$\sigma\sigma_e$ ((J m^{-2})^2)	1.11×10^{-3}	9.85×10^{-4}
σ (J m^{-2})	1.41×10^{-2}	1.78×10^{-2}
σ_e (J m^{-2})	7.87×10^{-2}	5.53×10^{-2}
K_{gI}/K_{gII}	1.87	1.87
Parameters of input data		
n	4	2
a_0 (nm)	0.463	0.651
b_0 (nm)	0.478	0.566
$\Delta h_f \times 10^{6a}$ (J m^{-3})	273.4	267.3
T_m^0 (K)	569	569
T_g (K)	390	390
U^* (J/mol)	6300	6300

[a] Heat of fusion per unit volume was calculated by using the densities of each crystal modification (1.407 g cm^{-3} for α-form and 1.439 g cm^{-3} for β-form) and heat of fusion per unit mass, $\Delta H_f = 190$ J g^{-1}, in Ref. [7] ($\Delta h_f = \Delta H_f \times \rho_c$).

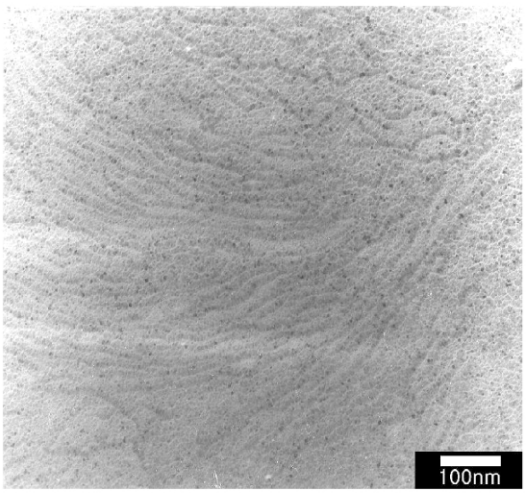

(a)

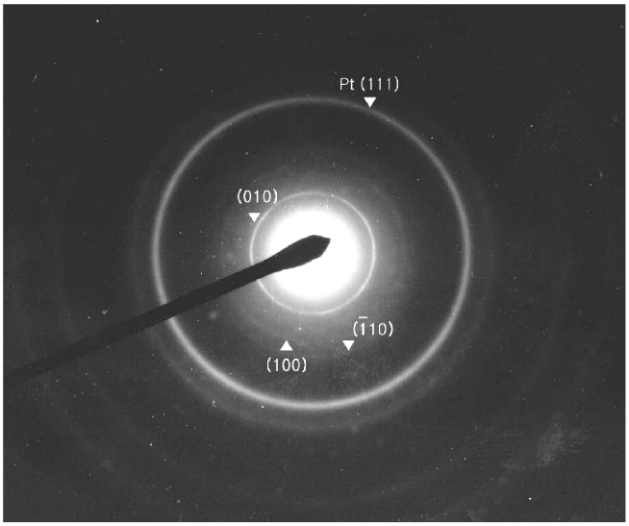

(b)

Fig. 10. (a) TEM images and (b) electron diffraction patterns taken from ultra-thin PEN films crystallized at 200 °C for 24 h.

On the other hand, the morphology of the β-modification shows rather different features as compared with that of the α-form crystals in Fig. 10. Fig. 11 presents the TEM images of the ultra-thin PEN films, melted at 300 °C and crystallized at 240 °C for 24 h. Fig. 11(a) shows crystalline lamellae, which is oriented in unique direction, like a sheaf. It has been reported that the β-form crystals form more dense crystals than α-form crystals, owing to higher packing density of the main-chain backbone. In our observation, β-form crystals with more dense packing of naphthalene rings showed an axialite structure, which was supposed to be the amoeba-type morphology observed in POM. Fig. 11(b) exhibits an electron diffraction pattern taken from the same

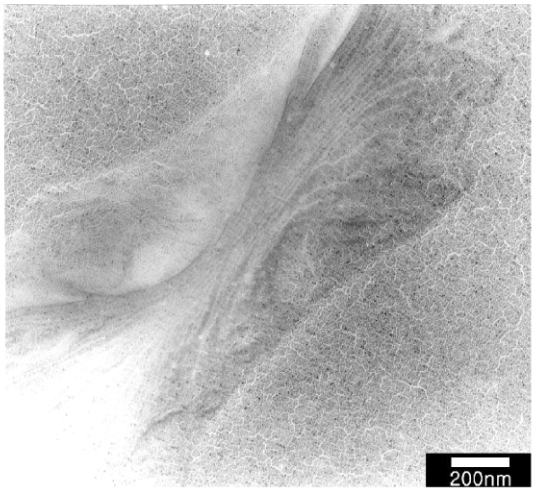

(a)

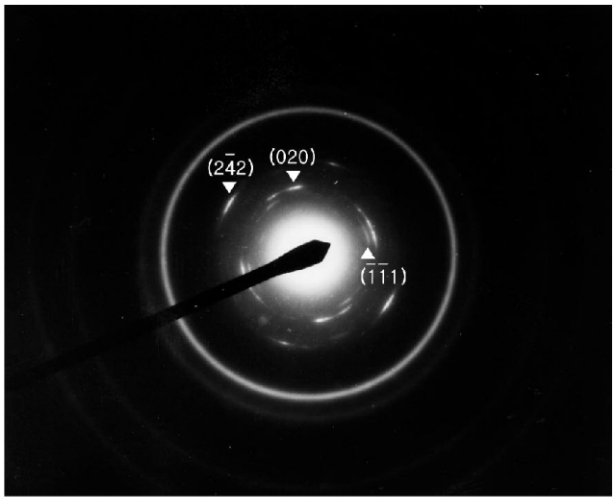

(b)

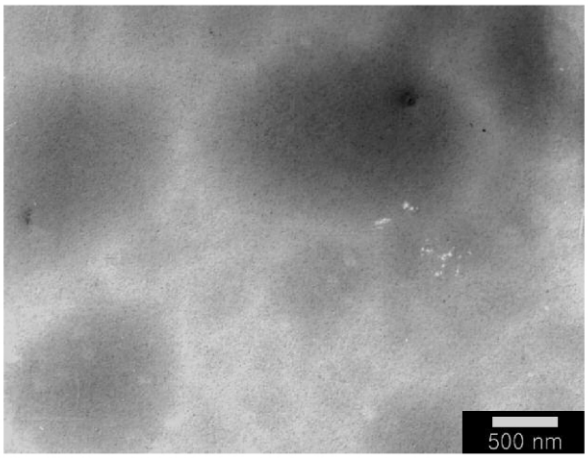

(c)

Fig. 11. (a), (c) TEM images and (b) electron diffraction patterns taken from ultra-thin PEN films crystallized at 240 °C for 24 h.

specimen. The electron diffraction patterns shown in Fig. 11(b) are the most common pattern in the ultra-thin PEN film crystallized at 240 °C. Crystalline reflections of the ($\bar{1}\bar{1}$1), (020), and (2$\bar{4}$2) planes, which are characteristic reflections to identify the β-form crystal, are clearly observed. Simultaneously, the (100) diffraction plane was observed obscurely. All the crystalline reflections in Fig. 11(b) are shown as a spot-like streak. This indicates that molecular chains of β-form crystals are oriented well to a given direction.

In spite of the long crystallization time (about 24 h), amorphous regions that did not take part in the crystallization were also observed in the same specimen, as shown in Fig. 11(c). In addition, when the ultra-thin PEN film was crystallized at 240 °C, electron diffraction results showed only β-form diffraction patterns. It is supposed that a seed is required for crystallization at 240 °C in the ultra-thin film system, and though the seeds exist, crystals do not grow into fully-developed spherulites due to the very low molecular concentration of the ultra-thin film. This means that crystallization in ultra-thin film advances only to the beginning of the crystallization process. Accordingly, we inferred that the initiation of the crystallization of PEN at 240 °C generates only β-form crystals. When PEN crystallized at 240 °C in bulk film, however, both α and β-form crystals coexisted as confirmed by the POM and WAXD results. It is supposed that not only thermal fluctuation may have occurred, but also many more options to nucleate the α-form could be possible in the bulk system.

4. Conclusions

The crystallization behavior and morphology of PEN were investigated by means of DSC, POM, and TEM.

1. Observation by POM revealed that PEN crystallized at 240 °C showed the coexistence of α and β-form spherulite morphologies with different growth rates. In addition, when PEN crystallized at 250 °C, the morphology of spherulites showed a squeezed peanut shape.
2. The Avrami exponents decreased from 3 to 2.8 above a T_c of 220 °C, indicating decrease of growth dimension. According to analysis based on secondary nucleation theory, PEN crystallized at 240 °C has crystals with both regime I and regime II, which means the axialitic and spherulitic growth forms. From the calculations of lateral and fold surface free energy, the nucleus shape of the β-form in regime I is more fibrous than that of the α-form in regime II.
3. In TEM observation, the ultra-thin PEN films crystallized at 200 °C showed a spherulitic texture with characteristic diffractions of the α-form. Ultra-thin PEN films crystallized at 240 °C produced an axialite structure with only β-form diffraction patterns. In addition, amorphous regions were also observed despite

long crystallization times. It is supposed that the initiation of crystallization of PEN at 240 °C generates only β-form crystals from axialite structures.

Acknowledgements

This work was supported by Hanyang University, Korea, in the program year of 2001, and was also supported by the Brain Korea 21 Project.

References

[1] Ouchi I, Noda H. Sen'i Gakkaishi 1973;29:405.
[2] Nakamae K, Nishino T, Tada K, Kanamoto T, Ito M. Polymer 1993; 34:3322.
[3] Van Den Heuvel CJM, Klop EA. Polymer 2000;41:4249.
[4] Uchida Y. Nikkei Mater Technol 1994;137:63.
[5] Mencik Z. Chem Prum 1967;17:78.
[6] Zachmann HG, Wiswe D, Gehrke R, Riekel C. Makromol Chem Suppl 1985;12:175.
[7] Buchner S, Wiswe D, Zachmann HG. Polymer 1989;30:480.
[8] Kim SJ, Nam JY, Lee YM, Im SS. Polymer 1999;40:5623.
[9] Cakmak M, Wang YD, Simhambhatla M. Polym Engng Sci 1990;30: 721.
[10] Murakami S, Nishikawa Y, Tsuji M, Kawaguchi A, Kohjiya S, Cakmak M. Polymer 1995;36:291.
[11] Cakmak M, Lee SW. Polymer 1995;36:4039.
[12] Murakami S, Yamakawa M, Tsuji M, Kohjiya S. Polymer 1995;37: 3945.
[13] Nilno H, Yabe A, Nagano S, Miki T. Appl Phys Lett 1989;54:2159.
[14] Tsuji M, Fernando A, Novillo L, Fujita M, Murakami S, Kohjiya S. J Mater Res 1999;14:251.
[15] Lee SW, Cakmak M. J Macromol Sci Phys 1998;B37(4):501.
[16] Liu J, Sidoti G, Hommema JA, Geil PH, Kim JC, Cakmak M. J Macromol Sci Phys 1998;B37(4):567.
[17] Plummer CJG. Macromol Rapid Commun 1999;20:157.
[18] Cheng SZD, Wunderlich B. Macromolecules 1988;21:789.
[19] Avrami M. J Chem Phys 1941;9:177.
[20] Hoffman JD, Davis GT, Lauritzen JI. In: Hannay NB, editor. Treatise on solid state chemistry: crystalline and non-crystalline solids, vol. 3. New York: Plenum Press; 1976.
[21] Thomas DG, Stavely LAK. J Chem Soc 1952;4569.
[22] Daubeny R De P, Bunn CW. Proc R Soc London A 1954;226:531.
[23] Wunderlich B, Macromolecular physics: crystal nucleation, growth, annealing, vol. 3. New York: Academic Press; 1976.